FIV2024
IGUAÇU FALLS, BRAZIL
2-5 JULY 2024

FIV2024: FSI² & FIV + N
10th International Symposium on Fluid-Structure Interactions,
Flow-Sound Interactions, Flow-Induced Vibration & Noise

FIV2024-0058
A REDUCED-ORDER MODEL OF 3-D EXTENSIBLE PIPES CONVEYING FLUID: AN APPROACH VIA A MODULAR BASED STRATEGY

Daniel de Oliveira Tomin
Celso Pupo Pesce
Renato Maia Matarazzo Orsino
Offshore Mechanics Laboratory, Escola Politécnica, University of São Paulo, Av. Professor Lúcio Martins Rodrigues, Tv. 4, n. 434, São Paulo - SP, 05508-020, Brazil
daniel.tomin@usp.br, ceppesce@usp.br, reorsino@usp.br

Abstract. *The slender flexible pipe is a basic structural element of pipeline transport systems that achieves an important role in the energy transition of the modern hydrocarbon industry. Pipe interactions with fluid flows are a main topic in Fluid-Structure Interactions research, including the dynamic behavior under internal flow. The present paper proposes 3-D nonlinear reduced-order models of inextensible and extensible cantilevered pipes conveying fluid subjected to static drag forces due to external flow, that satisfy the fundamental conditions of mass conservation and considers ejection or aspiration regimes. The modeling treats an open system whose dynamics is characterized by Hopf bifurcations and a critical internal velocity threshold. Furthermore, the models are derived by applying the extended Hamilton's Principle for nonmaterial volumes along with the Modular Modeling Methodology. Through a recursive algorithm, this strategy enables the treatment of nonlinearities by introducing redundant variables that simplify the derivation and reduce the number of mathematical operations. The aim is to elaborate an initial parametric study on the influence of extensibility though Argand's type diagrams that are obtained with the linearized versions of the equations of motion, that considers each static equilibrium position iteratively.*

Keywords: *Fluid-structure interactions, reduced-order modeling, pipe conveying fluid, Modular Modeling Methodology*

1. INTRODUCTION AND OBJECTIVES

The vibration introduced by the axial internal flow in flexible pipes is one of the main topics of scientific development in Fluid-Structure Interactions (FSI) research and has been described as a new paradigm in dynamics, comparable to the buckling of a beam under compressive load due to the fundamental aspects of its dynamical behavior (see Païdoussis and Li (1993)). According to the magnitude of the internal flow velocity, the steady state response of the system changes from stability around the static equilibrium configuration to a limit cycle characterized by a dynamic Hopf bifurcation, defining a critical flow velocity threshold. It is an inherent nonconservative and open system, in which complementary terms related to material transport must be considered in order to obtain the correct mathematical formulation.

As such, this problem was a catalyst for the derivation of extended variational principles of Analytical Mechanics for variable mass systems or nonmaterial volumes (*control volumes*). The generalized closed-form expressions of the Euler-Lagrange Equations and Hamilton's Principle have been obtained in Irschik and Holl (2002) and Casetta and Pesce (2013), respectively, highlighting not only the presence of a term of transport of momentum through the open boundary, but also a previously unknown term related to the transport of kinetic energy. The latter term has not been extensively considered in the modeling of the pipe conveying fluid; however, under the hypothesis of inextensiblity and plug flow, Kheiri and Païdoussis (2014) proved that this term is identically null.

One of the main practical application of the modeling of this phenomenon includes the global dynamics of risers. Risers are tubular, long and flexible structures that connect floating production storage and offloading units (FPSOs) to oil or gas production wells. In particular, the Seawater Intake Risers (SWIRs) under aspiration regimes, transport deep cold water with the objective of decreasing the carbon emissions of FPSOs plant cooling systems. Besides, another potential application is in excavation sites for carbon dioxide or hydrogen storage in salt rock domes, in which flexible pipes under strong ejection instabilities are utilized. This strategy is an essential solution in meeting the increasing demands of global activities, promoting renewable energy resources. Both of these examples highlight the importance of the problem in the energy transition for the modern offshore hydrocarbon industry.

The Offshore Mechanics Laboratory (LMO) research team has carried out several theoretical studies and experimental campaigns of FSI problems in risers. In the context of analytical modeling, the Modular Modeling Methodology (MMM) - initially developed for discrete multibody systems by Orsino (2016) and Orsino (2017) - has been utilized successfully in the analysis of pipes conveying fluid though consistent variational principles (such as Orsino *et al.* (2021) and Tomin (2022)). In continuous systems, the MMM algorithm is combined with a discretization scheme that assumes the definition of the so-called redundant variables as constraints, simplifying the algebraic manipulation of nonlinear terms.

The purpose of this work is the development of a preliminary parametric study on the influence of the extensibility on the general dynamics of submerged three-dimensional cantilevered flexible pipes subjected to the simultaneous action of both axial internal flow and static drag forces due to external flow, considering inextensible and extensible formulations. A reduced-order modeling (ROM) approach based on the fundamental principles of Analytical Mechanics for open systems - under consistent conditions of conservation of mass for the internal fluid - along with the MMM is used. Initially, the stability of the system is evaluated with linearized versions of the equations of motion though Argand-type diagrams and Lyapunov's indirect method. The linearization procedure computes a distinct static equilibrium configuration for each value of the internal and external flow velocities, recalculating the eigenvalues iteratively. The natural periods are obtained as a function of the dimensionless internal velocity, and in later studies, will be utilized to characterize scenarios for numerical integrations that explore other FSI problems such as the resonant phenomenon of vortex-induced vibrations (VIV) induced by the external flow, considering the fluctuating hydrodynamic loads through a phenomenological modeling approach.

2. MODELING OF THE SUBMERGED PIPE CONVEYING FLUID UNDER STATIC DRAG FORCES

Consider a 3-D submerged slender cantilevered pipe conveying fluid under static drag forces and gravitational effects. The cantilevered end O is the origin of an inertial Cartesian coordinate system (x, y, z) with a positive orthonormal basis $(O, \hat{\mathbf{x}}, \hat{\mathbf{y}}, \hat{\mathbf{z}})$. The undeformed axial coordinate x_0 characterizes the reference position of the pipe centerline, whereas s is the arc-length coordinate. See Fig. 1.

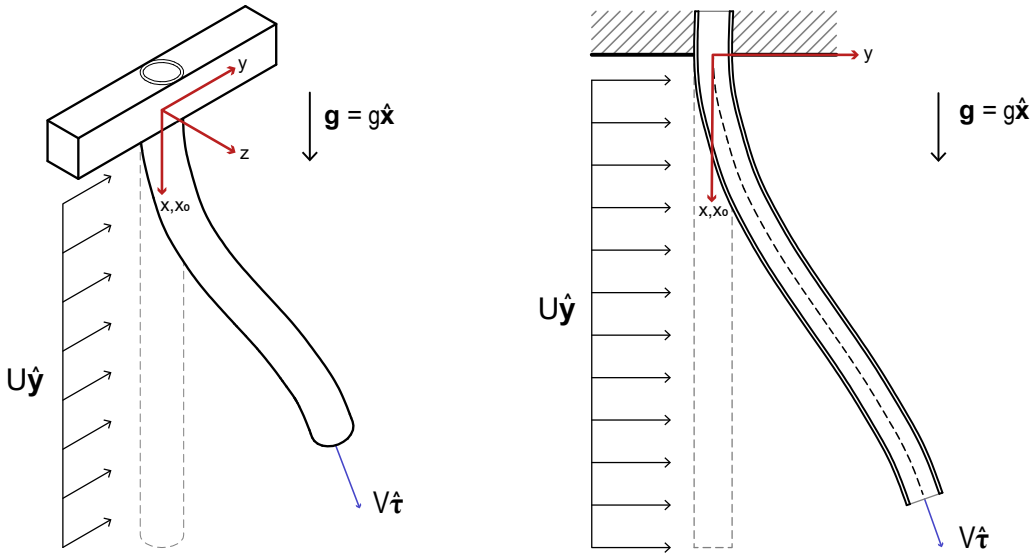

Figure 1: The 3-D model. The reference (vertical) configuration is shown by the gray dashed lines.

The assumptions made and the parameters of the pipe, internal and external fluids are as follows:

- Assume E is the Young's modulus, G the shear modulus, ν the Poisson's ratio, D the external diameter, d the internal diameter, $A = \pi\left(D^2 - d^2\right)/4$ the cross-sectional area, $a = \pi d^2/4$ the internal area, I_2 the second-order area moment of inertia, I_4 the fourth-order area moment of inertia, ρ_p the density, l the length and $m = \rho_p A$ the linear mass of the pipe. The acceleration of gravity is $\mathbf{g} = g\hat{\mathbf{x}}$.
- The internal flow velocity is given by $V\hat{\boldsymbol{\tau}}$, in which the magnitude V is calculated according to the essential conditions of conservation of mass in extensible formulations and $\hat{\boldsymbol{\tau}}$ is the centerline tangent unit vector. The internal fluid density is ρ_f and the linear mass is $M = \rho_f a$.
- The free-stream velocity is $U\hat{\mathbf{y}}$, the external fluid density is ρ_e, the linear mass displaced by the pipe is $m_d = \rho_e\left(A + a\right)$ and the added mass per unit length is $m_a = \rho_e\left(A + a\right)$ (under potential flow theory for circular cylinders).
- Assume t represents time, $\dot{(\,)} = \partial(\,)/\partial t$ and $(\,)' = \partial(\,)/\partial x_0$.

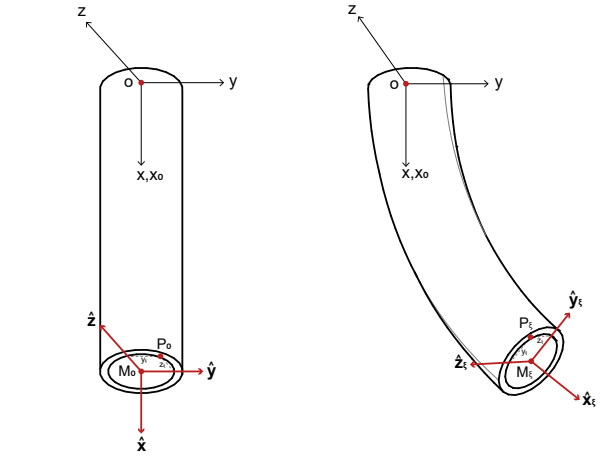

(a) Reference vertical configuration and a generic deformed position.

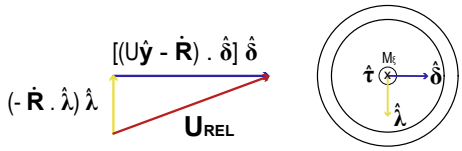

(b) Components of the relative external flow velocity $\mathbf{U}_{rel}$.

Figure 2: Definition of bases, vectors and parameters related to pipe motion.

2.1 Beam formulation and kinematics

Following Da Silva (1988), the cantilevered pipe is modeled as a straight slender Euler-Bernoulli beam made of an elastic linear material and considering bending, torsion and extensibility in a 3-D reference frame. Shear is disregarded and no cross-section warping is present (cylindrical pipe). Figure 2a shows the reference and deformed configurations of the pipe.

Before deformation ($t = 0$), the reference configuration is parallel to the $\hat{\mathbf{x}}$-axis and the local gravitational field. In a singular cross-section C_ξ, the centroid $M_\xi(t = 0) = M_0$ is the position of the pipe centerline. A Cartesian coordinate system (x_ξ, y_ξ, z_ξ) defined by a positive orthonormal basis $(M_\xi, \hat{\mathbf{x}}_\xi, \hat{\mathbf{y}}_\xi, \hat{\mathbf{z}}_\xi)$ is fixed locally at each C_ξ, initially aligned with basis $(O, \hat{\mathbf{x}}, \hat{\mathbf{y}}, \hat{\mathbf{z}})$. Therefore, basis $(M_\xi, \hat{\mathbf{x}}_\xi, \hat{\mathbf{y}}_\xi, \hat{\mathbf{z}}_\xi)$ is always composed of principal axes of inertia, and a material point $P_\xi(t = 0) = P_0$ of the pipe cross-section is always located in the corresponding $y_\xi z_\xi$-plane.

In a deformed state ($t > 0$), due to translational and rotational motion, points M_0 and P_0 move to generic positions $M_\xi(t)$ and $P_\xi(t)$. Three successive rotations are described using Euler angles: i) a rotation $\theta_z(t; x_0)$ along the $\hat{\mathbf{z}}$-axis, defining an intermediary basis $(M_\xi, \hat{\mathbf{x}}_1, \hat{\mathbf{y}}_1, \hat{\mathbf{z}}_1) = (M_\xi, \hat{\mathbf{x}}_1, \hat{\mathbf{y}}_1, \hat{\mathbf{z}})$; ii) a rotation $\theta_y(t; x_0)$ along the new $\hat{\mathbf{y}}_1$-axis, defining the basis $(M_\xi, \hat{\mathbf{x}}_2, \hat{\mathbf{y}}_2, \hat{\mathbf{z}}_2) = (M_\xi, \hat{\mathbf{x}}_2, \hat{\mathbf{y}}_1, \hat{\mathbf{z}}_2)$; iii) a final rotation $\theta_x(t; x_0)$ (angle of twist related to torsion) along the the new $\hat{\mathbf{x}}_2$-axis, defining the final basis $(M_\xi, \hat{\mathbf{x}}_3, \hat{\mathbf{y}}_3, \hat{\mathbf{z}}_3) = (M_\xi, \hat{\mathbf{x}}_2, \hat{\mathbf{y}}_3, \hat{\mathbf{z}}_3) = (M_\xi, \hat{\mathbf{x}}_\xi, \hat{\mathbf{y}}_\xi, \hat{\mathbf{z}}_\xi)$.

Let the displacements between points M_0 and $M_\xi(t)$ be $X\hat{\mathbf{x}} + Y\hat{\mathbf{y}} + Z\hat{\mathbf{z}} = (x - x_0)\,\hat{\mathbf{x}} + y\hat{\mathbf{y}} + z\hat{\mathbf{z}}$, the position vector of the centroid be $\mathbf{R} = (X + x_0)\,\hat{\mathbf{x}} + Y\hat{\mathbf{y}} + Z\hat{\mathbf{z}}$ and the axial strain ε be given by

$$\varepsilon = \frac{\mathrm{d}s - \mathrm{d}x_0}{\mathrm{d}x_0} = \sqrt{(1 + X')^2 + Y'^2 + Z'^2} - 1 \approx X' + \frac{1}{2}X'^2 + \frac{1}{2}Y'^2 + \frac{1}{2}Z'^2, \tag{1}$$

where $\mathrm{d}s$ and $\mathrm{d}x_0$ are, respectively, the infinitesimal lengths of the deformed and reference (vertical) configurations.

The tangent unit vector is

$$\begin{aligned}\hat{\boldsymbol{\tau}} &= \hat{\mathbf{x}}_\xi = \tau_x\hat{\mathbf{x}} + \tau_y\hat{\mathbf{y}} + \tau_z\hat{\mathbf{z}} \\ &= (\cos\theta_y \cos\theta_z)\,\hat{\mathbf{x}} + (\cos\theta_y \sin\theta_z)\,\hat{\mathbf{y}} + (-\sin\theta_y)\,\hat{\mathbf{z}}.\end{aligned} \tag{2}$$

It is important to note that the angular velocity vector $\boldsymbol{\omega}$, the linear mass moment of inertia tensor $\mathbf{J}$, and the curvature vector $\boldsymbol{\kappa}$ are expressed in terms of their components in the basis $(M_\xi, \hat{\mathbf{x}}_\xi, \hat{\mathbf{y}}_\xi, \hat{\mathbf{z}}_\xi)$ - the principal axes of inertia - in order to simplify the derivation of the equation of motion. It follows that

$$\begin{aligned}\boldsymbol{\omega} &= \omega_{x_\xi}\hat{\mathbf{x}}_\xi + \omega_{y_\xi}\hat{\mathbf{y}}_\xi + \omega_{z_\xi}\hat{\mathbf{z}}_\xi \\ &= \left(\dot{\theta}_x - \dot{\theta}_z \sin\theta_y\right)\hat{\mathbf{x}}_\xi + \left(\dot{\theta}_z \cos\theta_y \sin\theta_x + \dot{\theta}_y \cos\theta_x\right)\hat{\mathbf{y}}_\xi + \left(\dot{\theta}_z \cos\theta_y \cos\theta_x - \dot{\theta}_y \sin\theta_x\right)\hat{\mathbf{z}}_\xi,\end{aligned} \tag{3}$$

$$\mathbf{J} = \begin{bmatrix} \frac{2mI_2}{A} & 0 & 0 \\ 0 & \frac{mI_2}{A} & 0 \\ 0 & 0 & \frac{mI_2}{A} \end{bmatrix}, \tag{4}$$

$$\begin{aligned} \boldsymbol{\kappa} &= \kappa_{x_\xi}\hat{\mathbf{x}}_\xi + \kappa_{y_\xi}\hat{\mathbf{y}}_\xi + \kappa_{z_\xi}\hat{\mathbf{z}}_\xi \\ &= \left(\theta_x' - \theta_z' \sin\theta_y\right)\hat{\mathbf{x}}_\xi + \left(\theta_z' \cos\theta_y \sin\theta_x + \theta_y' \cos\theta_x\right)\hat{\mathbf{y}}_\xi + \left(\theta_z' \cos\theta_y \cos\theta_x - \theta_y' \sin\theta_x\right)\hat{\mathbf{z}}_\xi. \end{aligned} \tag{5}$$

In addition, accordingly with the Da Silva (1988) Euler-Bernoulli beam formulation, the following trigonometric expressions are valid:

$$\sin\theta_z \approx \frac{Y'}{1 + X' + \frac{1}{2}X'^2 + \frac{1}{2}Y'^2}, \;\; \cos\theta_z \approx \frac{1 + X'}{1 + X' + \frac{1}{2}X'^2 + \frac{1}{2}Y'^2}, \tag{6}$$

$$\sin\theta_y \approx \frac{-Z'}{1 + X' + \frac{1}{2}X'^2 + \frac{1}{2}Y'^2 + \frac{1}{2}Z'^2}, \;\; \cos\theta_y \approx \frac{1 + X' + \frac{1}{2}X'^2 + \frac{1}{2}Y'^2}{1 + X' + \frac{1}{2}X'^2 + \frac{1}{2}Y'^2 + \frac{1}{2}Z'^2}. \tag{7}$$

2.2 Internal flow and conservation of mass

The internal flow velocity $V\hat{\boldsymbol{\tau}}$ is tangential to the pipe centerline and modeled as plug flow. However, V cannot be assumed *a priori* as a constant parameter. Assume that $b = 1 - 2\nu$ is the volume change rate and V_0 is a constant value ($V_0 < 0$ and $V_0 > 0$ for aspiration and ejection regimes, respectively), the velocity field introduced in Ghayesh *et al.* (2013) for cantilevered extensible pipes is $V = (1 + \varepsilon)V_0/(1 + b\varepsilon)$.

In the present work, the authors propose a generalized expression for V based on propositions of extensibility and conservation of the internal fluid mass discussed by Tomin (2022). Consider Poisson's ratio $\nu = 0$ as in Euler-Bernoulli beam formulations and Eq. (1). By applying the principle of mass conservation for incompressible flows in an infinitesimal pipe length defined by a control volume $\mathcal{V}_u = \mathrm{d}s\, a$ (of external normal unit vector $\hat{\boldsymbol{\nu}}$) with the internal velocity at the inlet being V and the outlet $V + \mathrm{d}V = V + (\partial V/\partial x_0)\mathrm{d}x_0$, it follows that

$$\frac{\partial \mathcal{V}_u}{\partial t} + \int_{\partial \mathcal{V}_u} V\hat{\boldsymbol{\tau}} \cdot \hat{\boldsymbol{\nu}} \, \mathrm{d}\partial\mathcal{V}_u = 0 \;\; \rightarrow \;\; a\frac{\partial \varepsilon}{\partial t}\mathrm{d}x_0 + a\frac{\partial V}{\partial x_0}\mathrm{d}x_0 = 0 \;\; \rightarrow \;\; V = V_0 - \int_0^{x_0} \dot{\varepsilon}\, \mathrm{d}x_0; \tag{8}$$

The condition of mass conservation leads to a closed-form expression for V which is a function of the strain rate $\dot{\varepsilon}$; hence, V is a function of the generalized velocities of the problem. When inextensibility is assumed, the expression is reduced to $V = V_0$. For extensible modeling approaches based on Ghayesh *et al.* (2013), the internal flow velocity is only a function of ε and, specifically, is equal to $V = V_0$ if $\nu = 0$.

2.3 External flow

In order to define the drag forces due to external flow in each cross-section C_ξ and to enable a subsequent extended version of the current model through the inclusion of vortex-induced vibrations (VIV), an adaptation of the rigid cylinder VIV phenomenological model of Ogink and Metrikine (2010) presented in Orsino *et al.* (2021) is utilized.

Assume a constant free-stream velocity $\mathbf{U} = U\hat{\mathbf{y}}$. Let $\mathbf{U}_{rel}$ (magnitude U_{rel}) be the relative velocity between the external flow and the centroid M_ξ of each cross-section C_ξ. This relative velocity is related to the angle of attack Θ, which is measured from a new positive orthonormal basis composed of unit vectors $(M_\xi, \hat{\boldsymbol{\tau}}, \hat{\boldsymbol{\delta}}, \hat{\boldsymbol{\lambda}})$ of Fig. 2b. Consider $\hat{\mathbf{y}} \cdot \hat{\boldsymbol{\lambda}} = 0$, $\hat{\boldsymbol{\tau}} \cdot \hat{\boldsymbol{\lambda}} = 0$ and $\hat{\boldsymbol{\delta}} = \hat{\boldsymbol{\lambda}} \times \hat{\boldsymbol{\tau}}$. Thus, $\hat{\boldsymbol{\lambda}} = \lambda_x\hat{\mathbf{x}} + \lambda_z\hat{\mathbf{z}}$ and $\hat{\boldsymbol{\delta}} = \delta_x\hat{\mathbf{x}} + \delta_y\hat{\mathbf{y}} + \delta_z\hat{\mathbf{z}}$.

Proceeding with the phenomenological modeling, the force coefficients $\mathcal{C}_\delta$ and $\mathcal{C}_\lambda$ of the $\hat{\boldsymbol{\delta}}$ and $\hat{\boldsymbol{\lambda}}$ directions, respectively, can be written with the drag and lift coefficients - $\mathcal{C}_D$ and $\mathcal{C}_L$ - of stationary circular cylinders

$$\mathcal{C}_\delta = \frac{U_{rel}^2}{U^2}\left[\mathcal{C}_D \cos\Theta - \mathcal{C}_L \sin\Theta\right], \;\; \mathcal{C}_\lambda = \frac{U_{rel}^2}{U^2}\left[\mathcal{C}_D \sin\Theta + \mathcal{C}_L \cos\Theta\right], \tag{9}$$

in which

$$U_{rel} = \sqrt{\left[\left(U\hat{\mathbf{y}} - \dot{\mathbf{R}}\right) \cdot \hat{\boldsymbol{\delta}}\right]^2 + \left[-\dot{\mathbf{R}} \cdot \hat{\boldsymbol{\lambda}}\right]^2}, \;\; \sin\Theta = \frac{-\dot{\mathbf{R}} \cdot \hat{\boldsymbol{\lambda}}}{U_{rel}}, \;\; \cos\Theta = \frac{\left(U\hat{\mathbf{y}} - \dot{\mathbf{R}}\right) \cdot \hat{\boldsymbol{\delta}}}{U_{rel}}. \tag{10}$$

In Orsino *et al.* (2021), only a periodic lift coefficient is considered (related to a so-called oscillatory wake variable Q_n). Hence, $\mathcal{C}_D = C_D^0$ and $\mathcal{C}_L = (Q_n/\hat{Q})C_L^0$, where $\hat{Q} = 2$, C_D^0 is the mean drag coefficient and C_L^0 is the amplitude of the lift coefficient obtained from stationary data. Furthermore, $\mathcal{C}_\delta = c_\delta + C_\delta$ and $\mathcal{C}_\lambda = c_\lambda + C_\lambda$ may be separated into the following terms:

$$
\begin{aligned}
c_\delta &= C_D^0 \left(\hat{\mathbf{y}} \cdot \hat{\boldsymbol{\delta}}\right)^2, C_\delta = \frac{\sqrt{\left[\left(U\hat{\mathbf{y}} - \dot{\mathbf{R}}\right) \cdot \hat{\boldsymbol{\delta}}\right]^2 + \left[-\dot{\mathbf{R}} \cdot \hat{\boldsymbol{\lambda}}\right]^2}}{U^2} \left[C_D^0 \left[\left(U\hat{\mathbf{y}} - \dot{\mathbf{R}}\right) \cdot \hat{\boldsymbol{\delta}}\right] - \frac{Q_n}{\hat{Q}} C_L^0 \left[-\dot{\mathbf{R}} \cdot \hat{\boldsymbol{\lambda}}\right]\right] - c_\delta, \\
c_\lambda &= \frac{Q_n}{\hat{Q}} C_L^0 \left(\hat{\mathbf{y}} \cdot \hat{\boldsymbol{\delta}}\right)^2, C_\lambda = \frac{\sqrt{\left[\left(U\hat{\mathbf{y}} - \dot{\mathbf{R}}\right) \cdot \hat{\boldsymbol{\delta}}\right]^2 + \left[-\dot{\mathbf{R}} \cdot \hat{\boldsymbol{\lambda}}\right]^2}}{U^2} \left[C_D^0 \left[-\dot{\mathbf{R}} \cdot \hat{\boldsymbol{\lambda}}\right] + \frac{Q_n}{\hat{Q}} C_L^0 \left[\left(U\hat{\mathbf{y}} - \dot{\mathbf{R}}\right) \cdot \hat{\boldsymbol{\delta}}\right]\right] - c_\lambda.
\end{aligned}
\tag{11}
$$

In the context of the present study, no fluctuating VIV forces are assumed. Thus, the variables C_δ, c_λ and C_λ - associated with the wake variable Q_n - are not considered. Only the static parcel of the drag forces c_δ is utilized in the virtual work of the nonconservative forces.

3. EQUATIONS OF MOTION

Although Vectorial and Analytical Mechanics are well-established for classic problems comprising material volumes or closed systems, the formalisms are not straightforward when transport of mass occurs though an open boundary. In these cases, the definition of nonmaterial volumes $\mathcal{V}_u$ (*control volumes*) is important. They are fictitious volumes that instantly coincide with a certain region defined by the material particles. However, the surfaces $\partial\mathcal{V}_u$, associated with the external normal unit vector $\hat{\boldsymbol{\nu}}$, move at a different velocity than the material boundary; thus, transport of matter may exist.

McIver (1973)'s pioneering work applied Hamilton's Principle extended to variable mass systems, from which an additional term related to the transport of momentum was derived. Later, in Irschik and Holl (2002), the Euler-Lagrange Equations formalism was also extended to include nonmaterial volumes by applying the abstract concept of *fictitious particles*. However, the derivation in Irschik and Holl (2002) does not fully recover the formulation presented in McIver (1973). In fact, a term related to the transport of kinetic energy is missing. This inconsistency was resolved in Casetta and Pesce (2013), in which the extended Hamilton's Principle for nonmaterial volumes is derived

$$
\int_{t_1}^{t_2} \left[\delta L_u + \delta W_{NC} - \int_{\partial\mathcal{V}_u} \rho \, (\mathbf{v} \cdot \delta\mathbf{p}) \, (\mathbf{v} - \mathbf{u}) \cdot \hat{\boldsymbol{\nu}} \, \mathrm{d}\partial\mathcal{V}_u + \int_{\partial\mathcal{V}_u} \frac{1}{2} \rho \, (\mathbf{v} \cdot \mathbf{v}) \, (\delta\mathbf{p} - \delta\mathbf{r}) \cdot \hat{\boldsymbol{\nu}} \, \mathrm{d}\partial\mathcal{V}_u\right] \mathrm{d}t = 0, \tag{12}
$$

where t_1 and t_2 are instants of time t, L_u is the Lagrangian of the system and W_{NC} is the work of nonconservative forces. The density of the material (transported) particles is ρ, the virtual displacement is $\delta\mathbf{p}$ and $\mathbf{v} = \mathrm{d}\mathbf{p}/\mathrm{d}t$. The virtual displacement of the fictitious particles is $\delta\mathbf{r}$ and $\mathbf{u} = \mathrm{d}\mathbf{r}/\mathrm{d}t$ is equal to the velocity of the control surface. In comparison with closed systems, the complementary terms are: i) the third term - present in McIver (1973)'s derivation - is related to the transport of momentum; ii) the fourth term, associated with the transport of kinetic energy.

It is important to highlight that Irschik and Holl (2002) and Casetta and Pesce (2013) treat the variational principles in the spatial or Eulerian description of Continuum Mechanics. In Irschik and Holl (2015), the Euler-Lagrange Equations for open systems were derived in the framework of the material or Lagrange description, demonstrating their equivalence. A similar formulation of the Hamilton's Principle for open systems, however in the Lagrange description, appears to still be missing in the literature. This paper utilizes the material approach, consistently taking into account the nonmaterial volume and the terms related to the solid cantilever and the fluid flow, and dealing with moderately large pipe deformations.

The Lagrangian of the pipe conveying fluid is composed of the kinetic energy T_u and the potential energy P. The kinetic energy $T_u = T_p + T_f$ includes the pipe kinetic energy T_p (translational and rotational inertia) and that of the fluid particles T_f (translational inertia)

$$
T_p = \int_0^l \frac{m}{2} \left(\dot{\mathbf{R}} \cdot \dot{\mathbf{R}}\right) + \frac{1}{2} \left(\boldsymbol{\omega} \cdot \mathbf{J}\boldsymbol{\omega}\right) \, \mathrm{d}x_0, \;\; T_f = \int_0^l \frac{M}{2} \left[\left(\dot{\mathbf{R}} + V\hat{\boldsymbol{\tau}}\right) \cdot \left(\dot{\mathbf{R}} + V\hat{\boldsymbol{\tau}}\right)\right] \, \mathrm{d}x_0. \tag{13}
$$

The potential energy $P = P_g + P_s$ consists of the gravitational field P_g (including buoyancy effects) and strain energy P_s proposed in Da Silva (1988) simplified by the geometry of the cross-section, the definition of the principal axes of inertia $(M_\xi, \hat{\mathbf{x}}_\xi, \hat{\mathbf{y}}_\xi, \hat{\mathbf{z}}_\xi)$ and $G = E/2$ when $\nu = 0$, as follows:

$$
P_g = -\int_0^l (m + M - m_d) \, \mathbf{g} \cdot \mathbf{R} \, \mathrm{d}x_0, \tag{14}
$$

$$P_s = \int_0^l \frac{EA}{8}\left[1-2\left(1+\varepsilon\right)^2+\left(1+\varepsilon\right)^4\right] + \frac{EI_2}{8}\left[-2\kappa_{z_\xi}^2-2\kappa_{y_\xi}^2+\left(6\kappa_{z_\xi}^2+6\kappa_{y_\xi}^2+4\kappa_{x_\xi}^2\right)\left(1+\varepsilon\right)^2\right] + \frac{EI_4}{8}\left[\kappa_{z_\xi}^4+\kappa_{y_\xi}^4+2\kappa_{z_\xi}^2\kappa_{y_\xi}^2+\frac{8}{3}\kappa_{x_\xi}^2\left(\kappa_{z_\xi}^2+\kappa_{y_\xi}^2\right)+\frac{8}{3}\kappa_{x_\xi}^4\right]\,\mathrm{d}x_0. \tag{15}$$

The virtual work of the nonconservative forces δW_{NC} comprises the hydrodynamic loads, including added mass and drag forces

$$\delta W_{NC} = -\int_0^l m_a\ddot{\mathbf{R}}\cdot\delta\mathbf{R}\,\mathrm{d}x_0 + \int_0^l \frac{1}{2}\rho_e D U^2 c_\delta\hat{\boldsymbol{\delta}}\cdot\delta\mathbf{R}\,\mathrm{d}x_0. \tag{16}$$

Let q_i be the generalized coordinates of the discretized problem. The transport terms are only nonzero at the free end ($x_0 = l$)

$$\int_{\partial\mathcal{V}_u}\rho\,\left(\mathbf{v}\cdot\delta\mathbf{p}\right)\left(\mathbf{v}-\mathbf{u}\right)\cdot\hat{\boldsymbol{\nu}}\,\mathrm{d}\partial\mathcal{V}_u = \sum_{n=1}^{N} MV\left[\left(\dot{\mathbf{R}}+V\hat{\boldsymbol{\tau}}\right)\cdot\left(\frac{\partial\dot{\mathbf{R}}}{\partial\dot{q}_i}+\hat{\boldsymbol{\tau}}\frac{\partial V}{\partial\dot{q}_i}\right)\right]\,\delta q_i\Big|_{x_0=l}, \tag{17}$$

$$\int_{\partial\mathcal{V}_u}\frac{1}{2}\,\rho\,\left(\mathbf{v}\cdot\mathbf{v}\right)\left(\delta\mathbf{p}-\delta\mathbf{r}\right)\cdot\hat{\boldsymbol{\nu}}\,\mathrm{d}\partial\mathcal{V}_u = \sum_{n=1}^{N}\frac{M}{2}\frac{\partial V}{\partial\dot{q}_i}\left[\left(\dot{\mathbf{R}}+V\hat{\boldsymbol{\tau}}\right)\cdot\left(\dot{\mathbf{R}}+V\hat{\boldsymbol{\tau}}\right)\right]\,\delta q_i\Big|_{x_0=l}. \tag{18}$$

Notice that, Eq. (18) is identically zero in inextensible pipes ($\varepsilon = 0$) or extensible formulations based on internal velocity field expression proposed by Ghayesh *et al.* (2013), since $\partial V/\partial\dot{q}_i = 0$. Moreover, the terms of Hamilton's Principle are written in dimensionless form using the parameters listed in Tab. 1. In dimensionless expressions, assume $\dot{(\,)} = \partial(\,)/\partial\tau$, $(\,)' = \partial(\,)/\partial\xi$ and $\tilde{(\,)}$ to represent dimensionless quantities corresponding to the same symbol in previous equations.

Table 1: Dimensionless parameters.

Parameter	Symbol	Definition
Unstretched axial coordinate and displacements	$\xi, \eta, \vartheta, \zeta$	$\frac{x_0}{l}, \frac{X}{l}, \frac{Y}{l}, \frac{Z}{l}$
Time	τ	$\left(\frac{EI_2}{M+m}\right)^{1/2}\frac{t}{l^2}$
Internal and external flow velocities	v, u	$\left(\frac{M}{EI_2}\right)^{1/2}V_0 l, \left(\frac{M+m}{EI_2}\right)^{1/2}Ul$
Linear mass ratios	β, β_a, β_d	$\frac{M}{M+m}, \frac{m_a}{M+m}, \frac{m_d}{M+m}$
Axial and gravitational to flexural stiffness ratios	α, γ	$\frac{EA}{EI_2}l^2, \frac{M+m}{EI_2}gl^3$
Moment of inertia ratio	ψ	$\frac{EI_4}{EI_2 l^2}$
Inverse of the pipe aspect ratio	Δ	$\frac{D}{l}$

3.1 Modular Modeling Methodology

In order to apply the Modular Modeling Methodology algorithm, a preliminary ROM (called a *relaxed model*) is formulated with Galerkin's projection technique considering that, *a priori*, all the defined variables are independent, including the redundant ones shown in Tab. 2. This relaxed mode itself is not intended to represent the dynamics of the system, but to be used as a starting point for the derivation of the desired model. The angle of twist $\theta_x(\tau;\xi)$ is also disregarded in the derivations in this preliminary work.

The cantilevered end of the pipe implies that $\eta(\tau;\xi=0)=\vartheta(\tau;\xi=0)=\zeta(\tau;\xi=0)=\vartheta'(\tau;\xi=0)=\zeta'(\tau;\xi=0)=0$. Consequently, the nondimensional natural modes of a clamped-free Euler-Bernoulli beam - which identically satisfies these essential boundary conditions - are adopted for the discretization:

$$\Psi_n(\xi)=\cosh\Lambda_n\xi-\cos\Lambda_n\xi-\sigma_n(\sinh\Lambda_n\xi-\sin\Lambda_n\xi), \tag{19}$$

in which $\sigma_n=(\sinh\Lambda_n-\sin\Lambda_n)/(\cosh\Lambda_n+\cos\Lambda_n)$ and Λ_n is n-th value that results the characteristic equation $\cos\Lambda_n\cosh\Lambda_n=-1$. Consequently, $\Psi_n(0)=\Psi_n'(0)=\Psi_n''(1)=\Psi_n'''(1)=0$.

Table 2: Dimensionless redundant variables.

Variable	Expression
Axial strains	$\varepsilon=\eta'+\frac{1}{2}\eta'^2+\frac{1}{2}\vartheta'^2+\frac{1}{2}\zeta'^2, \varepsilon_p=\eta'+\frac{1}{2}\eta'^2+\frac{1}{2}\vartheta'^2$
Components of the tangent unit vector $\hat{\boldsymbol{\tau}}$	$\tau_x=\dfrac{1+\eta'}{1+\varepsilon}, \tau_y=\dfrac{\vartheta'}{1+\varepsilon}, \tau_z=\dfrac{\zeta'}{1+\varepsilon}$
Components of the curvature vector $\tilde{\boldsymbol{\kappa}}$	$\tilde{\kappa}_{x_\xi}=-\dfrac{\left[(1+\eta')\,\vartheta''-\vartheta'\eta''\right]\zeta'}{(1+\varepsilon_p)^2(1+\varepsilon)}, \tilde{\kappa}_{y_\xi}=\dfrac{\left[\zeta'\varepsilon_p'-(1+\varepsilon_p)\,\zeta''\right]}{(1+\varepsilon)^2}$ $\tilde{\kappa}_{z_\xi}=\dfrac{\left[(1+\eta')\,\vartheta''-\vartheta'\eta''\right](1+\varepsilon_p)}{(1+\varepsilon_p)^2(1+\varepsilon)}$
Components of the unit vector $\hat{\boldsymbol{\lambda}}$	$\lambda_x=\dfrac{-\tau_z}{\sqrt{\tau_x^2+\tau_z^2}}, \lambda_z=\dfrac{\tau_x}{\sqrt{\tau_x^2+\tau_z^2}}$
Components of the unit vector $\hat{\boldsymbol{\delta}}$	$\delta_x=-\tau_y\lambda_z, \delta_y=\tau_x\lambda_z-\tau_z\lambda_x, \delta_z=\tau_y\lambda_x$
Static parcel of the drag force coefficient	$c_\delta=C_D^0\left(\hat{\mathbf{y}}\cdot\hat{\boldsymbol{\delta}}\right)^2$
Components of the angular velocity vector $\tilde{\boldsymbol{\omega}}$	$\tilde{\omega}_{x_\xi}=-\dfrac{\left[(1+\eta')\,\dot{\vartheta}'-\vartheta'\dot{\eta}'\right]\zeta'}{(1+\varepsilon_p)^2(1+\varepsilon)}, \tilde{\omega}_{y_\xi}=\dfrac{\left[\zeta'\dot{\varepsilon}_p-(1+\varepsilon_p)\,\dot{\zeta}'\right]}{(1+\varepsilon)^2}$ $\tilde{\omega}_{z_\xi}=\dfrac{\left[(1+\eta')\,\dot{\vartheta}'-\vartheta'\dot{\eta}'\right](1+\varepsilon_p)}{(1+\varepsilon_p)^2(1+\varepsilon)}$
Internal velocity	$\tilde{V}=v\beta^{-1/2}-\displaystyle\int_0^\xi\dot{\varepsilon}\,\mathrm{d}\xi$

The original and the redundant variables are discretized as follows:

$$\begin{aligned}
&\eta(\tau;\xi)\cong\sum_{n=1}^{N}\Psi_n(\xi)\eta_n(\tau),\ \ \vartheta(\tau;\xi)\cong\sum_{n=1}^{N}\Psi_n(\xi)\vartheta_n(\tau),\ \ \zeta(\tau;\xi)\cong\sum_{n=1}^{N}\Psi_n(\xi)\zeta_n(\tau),\\
&\varepsilon(\tau;\xi)\cong\sum_{n=1}^{N}\Psi_n'(\xi)\varepsilon_n(\tau),\ \ \varepsilon_p(\tau;\xi)\cong\sum_{n=1}^{N}\Psi_n'(\xi)\varepsilon_{p_n}(\tau),\ \ \tau_x(\tau;\xi)\cong 1+\sum_{n=1}^{N}\Psi_n'(\xi)\tau_{xn}(\tau),\\
&\tau_y(\tau;\xi)\cong\sum_{n=1}^{N}\Psi_n'(\xi)\tau_{y_n}(\tau),\ \ \tau_z(\tau;\xi)\cong\sum_{n=1}^{N}\Psi_n'(\xi)\tau_{zn}(\tau),\ \ \tilde{\kappa}_{x_\xi}(\tau;\xi)\cong\sum_{n=1}^{N}\Psi_n''(\xi)\tilde{\kappa}_{x_\xi n}(\tau),\\
&\tilde{\kappa}_{y_\xi}(\tau;\xi)\cong\sum_{n=1}^{N}\Psi_n''(\xi)\tilde{\kappa}_{y_\xi n}(\tau),\ \tilde{\kappa}_{z_\xi}(\tau;\xi)\cong\sum_{n=1}^{N}\Psi_n''(\xi)\tilde{\kappa}_{z_\xi n}(\tau),\ \ \lambda_x(\tau;\xi)\cong\sum_{n=1}^{N}\Psi_n'(\xi)\lambda_{xn}(\tau),\\
&\lambda_z(\tau;\xi)\cong 1+\sum_{n=1}^{N}\Psi_n'(\xi)\lambda_{zn}(\tau),\ \ \delta_x(\tau;\xi)\cong\sum_{n=1}^{N}\Psi_n'(\xi)\delta_{xn}(\tau),\ \ \delta_y(\tau;\xi)\cong 1+\sum_{n=1}^{N}\Psi_n'(\xi)\delta_{y_n}(\tau),\\
&\delta_z(\tau;\xi)\cong\sum_{n=1}^{N}\Psi_n'(\xi)\delta_{zn}(\tau),\ \ c_\delta(\tau;\xi)\cong C_D^0+\sum_{n=1}^{N}\Psi_n'(\xi)c_{\delta n}(\tau),\ \ \tilde{\omega}_{x_\xi}(\tau;\xi)\cong\sum_{n=1}^{N}\Psi_n'(\xi)\tilde{\omega}_{x_\xi n}(\tau),\\
&\tilde{\omega}_{y_\xi}(\tau;\xi)\cong\sum_{n=1}^{N}\Psi_n'(\xi)\tilde{\omega}_{y_\xi n}(\tau),\ \ \tilde{\omega}_{z_\xi}(\tau;\xi)\cong\sum_{n=1}^{N}\Psi_n'(\xi)\tilde{\omega}_{z_\xi n}(\tau),\ \ \tilde{V}(\tau;\xi)\cong v\beta^{-1/2}+\sum_{n=1}^{N}\Psi_n(\xi)\tilde{V}_n(\tau).
\end{aligned} \tag{20}$$

Consider that $\mathbf{q}$ is the generalized coordinated vector. The discretized nonlinear equations of motion of the relaxed model are obtained in the following matrix form $\mathbf{M}(\tau;\mathbf{q};\dot{\mathbf{q}})\ddot{\mathbf{q}} = \mathbf{f}(\tau;\mathbf{q};\dot{\mathbf{q}})$ with the mass matrix $\mathbf{M}(\tau;\mathbf{q};\dot{\mathbf{q}})$ and the generalized forces vector $\mathbf{f}(\tau;\mathbf{q};\dot{\mathbf{q}})$. In the extensible model, the definitions of the redundant variables from Tab. 2 are interpreted as constraints that, after the Galerkin discretization, must be enforced in selected cross-sections C_ξ determined by the collocation points $\xi = \xi_n$. They are written in matrix form $\mathbf{A}_E(\tau;\mathbf{q};\dot{\mathbf{q}})\ddot{\mathbf{q}} = \mathbf{b}_E(\tau;\mathbf{q};\dot{\mathbf{q}})$. In the inextensible formulation, besides the expressions from Tab. 2, a complementary constraint equation related to inextensiblity is assumed, $\varepsilon = 0$. The matrix form is $\mathbf{A}_I(\tau;\mathbf{q};\dot{\mathbf{q}})\ddot{\mathbf{q}} = \mathbf{b}_I(\tau;\mathbf{q};\dot{\mathbf{q}})$. Let $\mathbf{S}_E(\tau;\mathbf{q};\dot{\mathbf{q}})$ and $\mathbf{S}_I(\tau;\mathbf{q};\dot{\mathbf{q}})$ be the projection operators whose images are correspondent to the kernels of the Jabobian matrices $\mathbf{A}_E(\tau;\mathbf{q};\dot{\mathbf{q}})$ and $\mathbf{A}_I(\tau;\mathbf{q};\dot{\mathbf{q}})$, respectively.

The equations of motion for each model are

$$\begin{bmatrix}\mathbf{S}_E^\top\mathbf{M}\\ \mathbf{A}_E\end{bmatrix}\ddot{\mathbf{q}} = \begin{bmatrix}\mathbf{S}_E^\top\mathbf{f}\\ \mathbf{b}_E\end{bmatrix}, \quad \begin{bmatrix}\mathbf{S}_I^\top\mathbf{M}\\ \mathbf{A}_I\end{bmatrix}\ddot{\mathbf{q}} = \begin{bmatrix}\mathbf{S}_I^\top\mathbf{f}\\ \mathbf{b}_I\end{bmatrix}. \tag{21}$$

4. RESULTS

Since the static equilibrium configuration of the pipe is a function of both the dimensionless internal velocity v and the external velocity u, this work proposes a linearization procedure that utilizes these static points accordingly, enabling the calculation of the eigenvalues λ_i recursively. Argand-type diagrams of the natural periods $T_i = 2\pi/|\,\mathrm{Im}[\lambda_i]|$ as a function of v are obtained. The stability of the system is evaluated through the color scale that represents the values of $\mathrm{Re}[\lambda_i]$. The analyses are done with $N = 6$ projection functions for ejection regimes ($v > 0$) and the parameters of Tab. 3.

Table 3: Set of dimensionless parameters.

Parameter	Value	Parameter	Value	Parameter	Value	Parameter	Value
α	1000	C_D^0	1.1856	γ	100	β_d	0.4167
ϕ	0.001	Δ	0.02	β	0.2	β_a	0.4167

In Figs. 3 and 4, the numerical results of ejection regimes from inextensible and extensible formulations are presented.

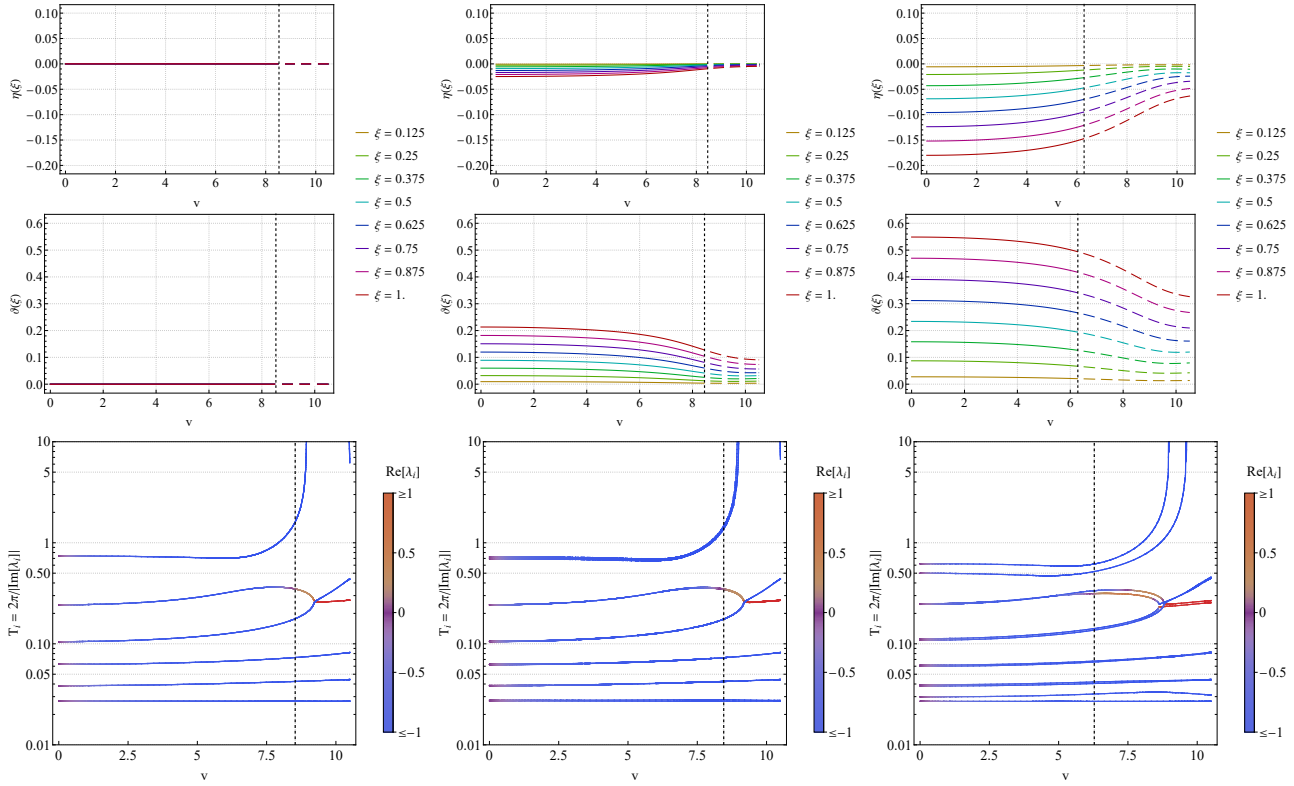

(a) $u = 0.$ $v_c = 8.5.$ (b) $u = 1.$ $v_c = 8.5.$ (c) $u = 2.$ $v_c = 6.3.$

Figure 3: Static configurations and root loci for the inextensible model.

The axial and transversal static displacements $\eta(\xi)$ and $\vartheta(\xi)$ (related to the y-direction) are displayed in several cross-sections of the pipe. The static transversal displacement $\zeta(\xi)$ (z-direction) is always zero. Also, in the inextensible root loci, the natural periods are associated with the transversal directions; whereas, in the extensible graphs, the axial natural periods are depicted besides the transversal values. Since there is symmetry between the two transversal directions, the curves associated with the transversal modes are the same for $u = 0$, and generally, are close for $u = 1$ and $u = 2$. The modes are classified at $v = 0$ according to the descending order of the natural periods T_i and the directions.

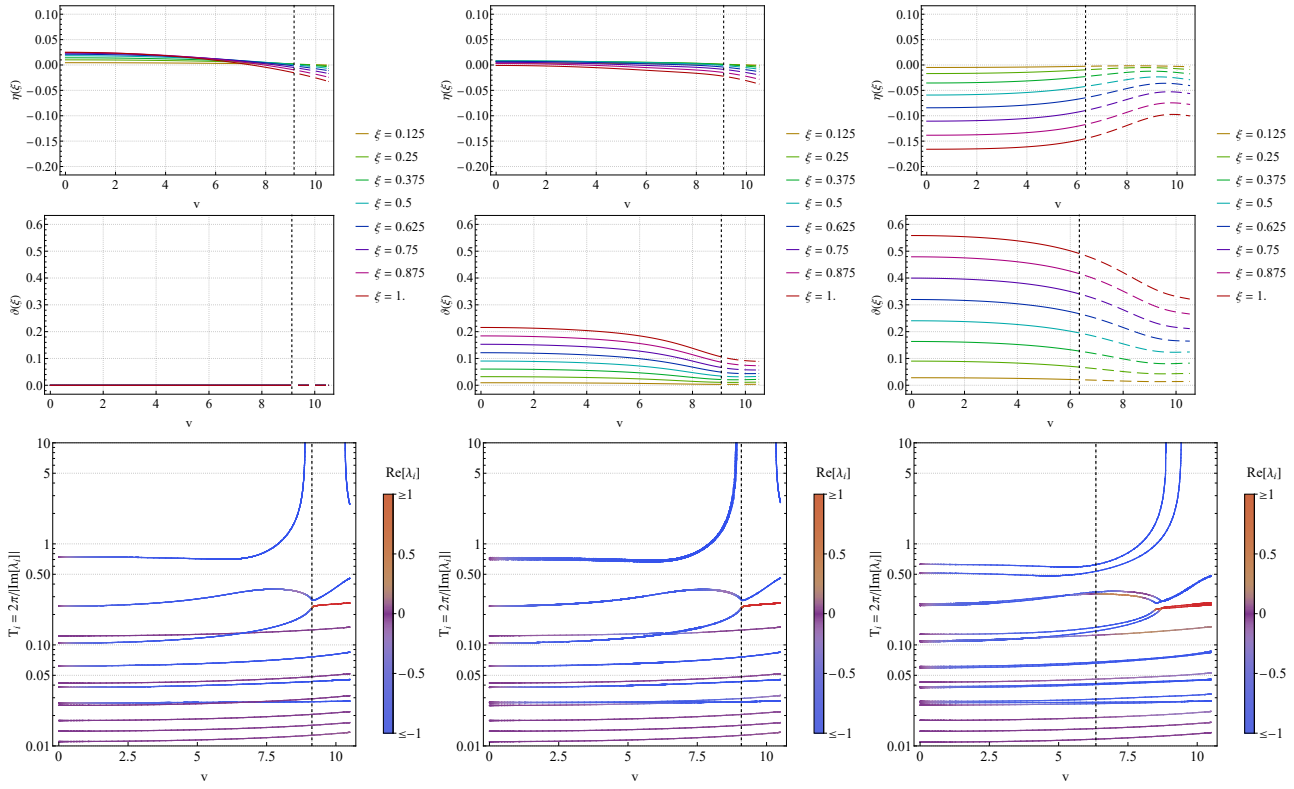

(a) $u = 0$. $v_c = 9.1$. (b) $u = 1$. $v_c = 9.1$. (c) $u = 2$. $v_c = 6.3$.

Figure 4: Static configurations and root loci for the extensible model.

For $u = 0$, it is possible to observe in the inextensible static configuration, that the system is in the reference vertical position. In the corresponding extensible graph, the transversal displacement is null; however, initially, in the axial direction, there is an elongation due to gravitational effects, followed by shortening for increasing v. In the inextensible root loci, the Hopf bifurcation appears in the second transversal mode and the critical velocity is $v_c = 8.5$. In the extensible root loci, the Hopf bifurcation appears in the third transversal mode and the critical velocity is higher, $v_c = 9.1$. Moreover, all the axial natural periods are relatively constant with low magnitude real parts. This case is similar to the planar ROM scenarios investigated in Tomin (2022). Assuming identical dimensionless parameters and $N = 8$ projection functions, the critical velocity is about $v_c = 10.6$ in the 2-D extensible discrete model presented in Ghayesh *et al.* (2013) when added mass and buoyancy effects are considered, higher than both the inextensible and extensible formulations proposed in this work.

For $u = 1$, the main difference between the models in the static configuration is related to the axial displacement. Due to the inextensibility condition, the values of $\eta(\xi)$ are negative and increase as v increases; however, in the extensible pipe, the values are, at first, positive and decrease when v increases. The root loci and critical velocities are similar to $u = 0$, even if the system loses symmetry as a consequence of the acting drag forces.

For $u = 2$, the static displacements are higher in magnitude and the qualitative behavior is the same between the inextensible and extensible pipes (even with relatively near values), mirroring the inextensible results for $u = 1$ of increasing static axial displacements as a function of v. In the root loci of the inextensible and extensible pipes, it is noticed that the transversal natural periods are distinct between the transversal directions (specially in the first and second modes), and the critical velocity is $v_c = 6.3$ for both models and related, initially, with a weak instability.

5. CONCLUDING REMARKS

In the present work, reduced-order models for the 3-D submerged cantilevered pipes conveying fluid are derived under extensible and inextensible formulations with the Modular Modeling Methodology; including the concomitant action of

the static drag forces due to external flow. This approach allows a degree of representativeness that is compatible with a detailed parametric study on the influence of the extensibility hypothesis in the dynamics of the problem.

As a classical problem of a variable mass system, the complementary terms related to material transport are accounted in the extended Hamilton's Principle for nonmaterial volumes generalized by Casetta and Pesce (2013). Under the essential conditions of extensibility and conservation of the internal fluid mass, it is possible to show the influence of the term of transport of kinetic energy through the open boundary, which is identically null in inextensible pipes. The modeling also utilized the nonlinear Euler-Bernoulli beam formulation of Da Silva (1988), that treats bending, torsion and extensibility, and includes already an adaptation proposed by Orsino *et al.* (2021) of the Ogink and Metrikine (2010) vortex-induced vibrations (VIV) phenomenological model to be tested in further time domain simulations.

In the numerical results, there is a significant distinct behavior between the inextensible and extensible formulations in the axial static configurations and the critical velocity for $u = 0$ and $u = 1$: i) under the inextensibility condition, the axial displacement is zero or negative, increasing as a function of v when $u = 1$; whereas, in the extensible pipe, the values are positive for $v = 0$, followed by a shortening when v increases; ii) the critical velocities are higher in the extensible model ($v_c = 9.1$) than the inextensible model ($v_c = 8.5$). Considering $u = 2$, the results from the static configurations and root loci are similar between the models, with identical qualitative behavior of the static configuration and the same critical velocity, $v_c = 6.3$. It is also possible to clearly observe different natural periods for the first and second modes of each transversal direction due to the drag forces in the y-direction. Later studies will propose VIV lock-in scenarios for numerical integrations in order to explore other capabilities of the present model.

ACKNOWLEDGEMENTS

The São Paulo State Research Foundation (FAPESP) is acknowledged, for having supported the whole development of the basic mathematical formalism, since 2012, through grants 2012/10848-4, 2013/02997-2, 2016/09730-0 and for the first author on-going PhD scholarship, 2023/03135-6, linked to the Thematic Project "Nonlinear Dynamics applied to Engineering Systems", process 2022/00770-0. C. Pesce acknowledges the National Council for Scientific and Technological Development (CNPq) research grant 307995/2022-4.

REFERENCES

Casetta, L. and Pesce, C.P., 2013. "The generalized Hamilton's principle for a non-material volume". *Acta Mechanica*, Vol. 224, No. 4, pp. 919–924. doi:10.1007/s00707-012-0807-9.

Da Silva, M.R.M.C., 1988. "Non-linear flexural-flexural-torsional-extensional dynamics of beams—I. Formulation". *International Journal of Solids and Structures*, Vol. 24, No. 12, pp. 1225–1234. doi:10.1016/0020-7683(88)90087-X.

Ghayesh, M.H., Païdoussis, M.P. and Amabili, M., 2013. "Nonlinear dynamics of cantilevered extensible pipes conveying fluid". *J. Sound Vib.*, Vol. 332, No. 24, pp. 6405–6418. ISSN 0022-460X.

Irschik, H. and Holl, H.J., 2002. "The equations of Lagrange written for a non-material volume". *Acta Mechanica*, Vol. 153, No. 3-4, pp. 231–248. doi:10.1007/BF01177454.

Irschik, H. and Holl, H.J., 2015. "Lagrange's equations for open systems, derived via the method of fictitious particles, and written in the Lagrange description of continuum mechanics". *Acta Mechanica*, Vol. 226, No. 1, pp. 63–79. ISSN 1619-6937.

Kheiri, M. and Païdoussis, M.P., 2014. "On the use of generalized Hamilton's principle for the derivation of the equation of motion of a pipe conveying fluid". *Journal of Fluid and Structures*, Vol. 50, pp. 18–24. ISSN 08899746. doi: 10.1016/j.jfluidstructs.2014.06.007.

McIver, D.B., 1973. "Hamilton's principle for systems of changing mass". *Journal of Engineering Mathematics*, Vol. 7, No. 3, pp. 249–261. doi:10.1007/BF01535286.

Ogink, R. and Metrikine, A., 2010. "A wake oscillator with frequency dependent coupling for the modeling of vortex-induced vibration". *Journal of Sound and Vibration*, Vol. 329, No. 26, pp. 5452–5473. doi:10.1016/j.jsv.2010.07.008.

Orsino, R.M.M., 2016. *A contribution on modeling methodologies for multibody systems*. Ph.D. thesis, University of São Paulo. doi:10.11606/T.3.2016.tde-22062016-160724.

Orsino, R.M.M., 2017. "Recursive modular modelling methodology for lumped-parameter dynamic systems". *Proceedings of the Royal Society A Mathematical, Physical and Engineering Sciences*, Vol. 473, No. 2204. doi: 10.1098/rspa.2016.0891.

Orsino, R.M.M., Pesce, C.P., Toni, F.G., Defensor Filho, W.A. and Franzini, G.R., 2021. "A 3D nonlinear reduced-order model of a cantilevered aspirating pipe under VIV". In *Advances in Nonlinear Dynamics: Proceedings of the Second International Nonlinear Dynamics Conference (NODYCON 2021), Volume 1*. Springer, Virtual, pp. 107–117.

Païdoussis, M.P. and Li, G.X., 1993. "Pipes conveying fluid: a model dynamical problem". *Journal of Fluids and Structures*, Vol. 7, No. 2, pp. 137–204. ISSN 0889-9746. doi:10.1006/jfls.1993.1011.

Tomin, D.O., 2022. *Dinâmica de tubos extensíveis com escoamento interno: uma abordagem via Mecânica Analítica*. Master's thesis, University of São Paulo. doi:10.11606/D.3.2021.tde-07102022-073508. In Portuguese.